High-order regime of harmonic generation with two active electrons

J. Prager,* S. X. Hu,† and C. H. Keitel‡
Theoretische Quantendynamik, Fakultät für Physik, Albert-Ludwigs-Universität Freiburg, Hermann-Herder-Straße 3, D-79104 Freiburg, Germany
(Received 21 May 2001; published 10 September 2001)

The influence of a second active electron is studied in the high-order regime of nonrelativistic harmonic generation in model helium. The major deviation of the harmonic yield due to the second active electron is small and associated mostly with the descreening of the helium nucleus while only an even smaller part remains as a consequence of the electron-electron repulsion.

DOI: 10.1103/PhysRevA.64.045402 PACS number(s): 42.50.Hz, 31.30.Jv, 32.80.Rm

Atomic gases and solids in very intense laser pulses may give rise to high harmonics of the applied laser frequency [1]. This process is thus of interest as a source of coherent high-frequency light and has been studied extensively and understood rather well within the so-called single active electron model that neglects dynamical electron correlation [2,3]. While the topic of nonsequential double ionization in intense laser fields has been investigated extensively for several years, the process of harmonic generation played little role in the discussion of possible signatures of electron correlation in strong laser pulses. This is easily understood, since measurements of the double ionization yield revealed discrepancies of several orders of magnitude as compared to predictions based on single active electron models [4].

In the case of harmonic generation, the question of correlation effects arose from a measurement of Sarukura *et al.* [5] who observed up to the 23rd harmonic emitted by helium atoms driven by a KrF laser (248 nm wavelength). After it was suggested that the He^+ ion should contribute to the harmonic yield near the saturation intensity [6], a calculation that included the weighted contribution of the ion to the spectrum within a single active electron approximation fitted the experimental data quite remarkably [7,8]. Another calculation that was based on explicitly correlated basis functions matched the data also very well [9]. Furthermore, employing an improved density-functional theory it was found that both dynamical correlation and the contribution of He^+ are responsible for the highest harmonics, and it was added that these two explanations are related to each other [10]. In the continued discussion, it was then reported that with a suitably short turn on of the laser pulse the emission of the highest harmonics could be attributed to the helium atom, i.e., not necessarily to the ion [11]. In the lower-frequency tunneling regime similar, but somehow, less pronounced results were found [6,8,10]. Several additional calculations from fully correlated one-dimensional treatments [12] to benchmark simulations in full 3D on a parallel supercomputer [13] confirmed the deviations in the harmonic yield due to the involvement of two correlated active electrons though with some differences in the precise amount. Most of those considerations, however, were associated with the multiphoton regime or the beginning of the tunneling regime and less attention was paid to the regime of very high-harmonic generation. In this situation, the tunneled electron spends little time in both the vicinity of the nucleus and the bound second electron, while the oscillation amplitude of the bound inner electron is enhanced.

In this Brief Report, we investigate low-frequency high-harmonic generation with laser intensities beyond $10^{15}\ \mathrm{W\,cm^{-2}}$ where hundreds of harmonics with rather small influence of correlation arise. We evaluate the total deviation of the harmonic yield due to the second active electron including the influence of the magnetic-field component of the laser field. Via an evaluation of the effective potential of ion and inner electron the main fraction of the deviation is shown to be associated with the descreening of the ionic core. A small fraction though remains for electron correlation, which we consider also via the evaluation of the momentum distribution of the recolliding electron with one and two active electrons.

Due to the smallness of the correlation, we employ the Hartree-Fock picture [2,14] of the wave function for the helium atom $\psi(\boldsymbol{r}_1,\boldsymbol{r}_2,t)$ being approximated by the product of a doubly occupied orbital ϕ

$$\psi(\boldsymbol{r}_1,\boldsymbol{r}_2,t)=\phi(\boldsymbol{r}_1,t)\,\phi(\boldsymbol{r}_2,t),$$

with $\boldsymbol{r}_1$ and $\boldsymbol{r}_2$ being the position coordinates of the two electrons and t the time. We then consider the following Schrödinger equation beyond the dipole approximation (in atomic units as throughout this paper)

$$i\partial_t\phi(\boldsymbol{r},t)=\left[H_0+\frac{\langle\phi|H_1|\phi\rangle}{\langle\phi|\phi\rangle}\right]\phi(\boldsymbol{r},t).$$

Here, H_0 is the single-electron Hamilton operator with spatial coordinate $\boldsymbol{r}$ (y is the component in the laser propagation direction) and electron momentum $\boldsymbol{p}$, while H_1 contains the interaction of the electrons:

$$H_0=\frac{\boldsymbol{p}^2}{2}+\frac{1}{c}\boldsymbol{A}(\boldsymbol{y},t)\cdot\boldsymbol{p}+\frac{1}{2c}\boldsymbol{A}^2(\boldsymbol{y},t)+V_0(\boldsymbol{r}),$$

$$H_1=V_1(|\boldsymbol{r}_1-\boldsymbol{r}_2|).$$

*Email address: prager@uni-freiburg.de
†Present address: Department of Physics and Astronomy, University of Nebraska–Lincoln, Lincoln, NE 68588-0111. Email address: shu@unlnotes.unl.edu
‡Email address: keitel@uni-freiburg.de

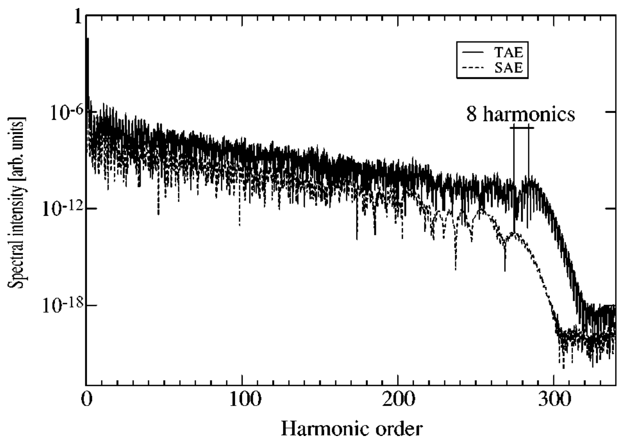

FIG. 1. Harmonic yield obtained with the single active electron (SAE) approximation and with two active electrons (TAE). The intensity employed is 2.19×10^{15} W cm^{-2} at a laser wavelength of 780 nm.

As usual, $\boldsymbol{A}$ denotes the vector potential of the external electromagnetic field, while c stands for the speed of light. To stabilize the numerical computations, we choose for the interaction with the atomic core V_0 and between the electrons V_1, the well-established soft core potential [15] $V_{0,1}(\boldsymbol{r}) = k_{0,1}/\sqrt{|\boldsymbol{r}|^2 + a_{0,1}}$. This introduces four parameters that are adapted such that both numerical stability and the correct ground eigenstates of He^+ (-2.0) and He (-2.9) are approximately reproduced: $a_0 = 1.0$, $a_1 = 0.15$, $k_0 = -3.28$, $k_1 = 1.2$. We solve the Schrödinger equation directly on a two-dimensional grid involving the polarization and the propagation directions with the so-called split-operator method [16,17]. The grid size is 409.6 and 102.4 a.u. in the polarization and the propagation direction, respectively, with a spacing of 0.2 a.u. In order to prevent parts of the wave function from being reflected from the edges, an absorbing boundary is used. We produce the initial wave function with a combination of the propagation in imaginary time and the spectral method [17]. Finally, the pulse shape employed here consists of a five cycle linear turn on followed by five cycles at constant amplitude. We do not consider a turn off here, because it is of no importance for the position of the highest harmonics of interest here. The pulse is chosen short because the high-ionization probability for the parameters employed here would render the emission of harmonics less effective with a longer pulse. The spectral intensity I that is emitted in the laser propagation direction y can be calculated from the dipole acceleration a_x in the polarization direction x with the help of a Fourier transformation

$$I \propto \left| \int_{-\infty}^{\infty} a_x(t) e^{i\omega t} dt \right|^2,$$

where the average dipole acceleration of each electron is obtained via Ehrenfest's theorem

$$a_x(t) = \left\langle \phi \left| -\frac{\partial}{\partial x}\left(V_0 + \frac{\langle \phi | V_1 | \phi \rangle}{\langle \phi | \phi \rangle} \right) \right| \phi \right\rangle.$$

In Fig. 1, we show the radiation spectrum via the Hartree-Fock model with two active electrons (TAE) in comparison with the result obtained in the single active electron approximation (SAE). Both spectral yields have the same principal features involving harmonics with plateau and cutoff. In the case of the single active electron, the highest harmonics in the cutoff region are few orders of magnitude less intense than in the two electron case. Furthermore, with inclusion of the dynamics of the second electron, the cutoff frequency is placed at about eight harmonics higher as compared to the situation with a single active electron. With respect to the expected cutoff frequency at the 271th harmonic for laser-driven helium at the chosen laser parameters, the difference is small but clearly originates from taking into account the second electron. In agreement with former results [18,10,13] in a different parameter regime, our calculations show that the single active electron model exhibits a significantly higher-ionization rate than with the inclusion of the second electron near the saturation intensity. As will be shown also in our parameter regime, this is mostly understood via dynamical screening, i.e., the lack of descreening of the nucleus via the moving inner electron, which also leads to less intense harmonics in the SAE case.

In order to determine the times when the highest harmonics are emitted, we employ a window function on the Fourier transformed dipole acceleration so that only the harmonics in the cutoff region remain. Afterwards, we carry out the inverse Fourier transformation. This way we find that after the turnon (five cycles) the periodic emission of the cutoff harmonics takes place at times in agreement with the recollision model [3,19,20]. Due to the high-ionization probability in the SAE case, intense emission of the highest harmonics takes place mainly a short time after the turn on of the laser pulse around 5.45 cycles. We note that the recollision times with SAE and TAE differ only by 0.0003 laser cycles, an indication already that electron correlation has only little effect on electron tunneling, free electron motion in the laser field and the recollision, i.e., may not be responsible for the main contribution of the additional eight harmonics.

Following the scaling law of the recollision model, the ionization potential contributes as does the electron energy at the time of the recollision. In the TAE case, the effective potential sensed by the recolliding electron is time dependent due to the motion of the inner electron. In Fig. 2, we display the effective potential experienced by the tunneled electron exactly at the time of maximal emission of the cutoff harmonics after 5.45 cycles. The ground-state energies of the effective potentials are calculated to be -1.03 and -1.37 a.u. for the SAE and TAE situation, respectively. From the scaling law for the cutoff frequency $I_p + 3.17\,U_p$ this difference in I_p alone can only explain six of the eight harmonics more in the spectrum with two active electrons.

In order to investigate the role of dynamical correlations, we show in Fig. 3 the momentum distribution of the tunneled electron at the time of maximal emission of the highest harmonics at 5.45 cycles. To eliminate the change in momentum due to the recombination process, i.e., the Coulomb potential, we smoothly turned off the core potential starting at the beginning of the 5th cycle. This way, we make sure that the tunneling process, that takes place at ca. 4.75 cycles, is un-

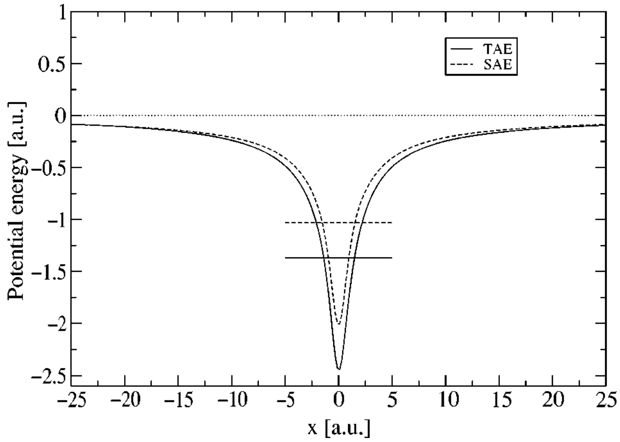

FIG. 2. Effective potential as jointly formed by the Coulomb fields of the ion and the electron repulsion and the ground-state energies for the TAE and SAE models after 5.45 cycles, i.e., at the time of maximal emission of the highest harmonics. The ground-state energies lie at -1.37 a.u. (TAE) and -1.03 a.u. (SAE).

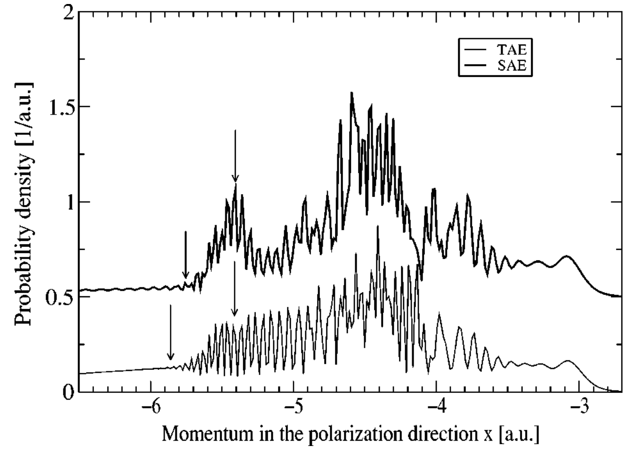

FIG. 3. Momentum distribution in the polarization direction of the recolliding electron at the time of maximal emission of the highest harmonics after 5.45 cycles. For clarity, for the SAE case, the distribution was shifted 0.5 a.u. upwards.

altered. Differences in the momentum distribution between the SAE and TAE model would come solely from an influence of the second moving bound electron on the tunneling process or the quasifree electron propagation. In Fig. 3, we placed two arrows in each plot indicating the minimal and maximal momenta of the recolliding electron that would be necessary to produce the observed harmonics in the cutoff region. The limits were obtained using the scaling law of the recollision picture $p=\sqrt{2(\omega-I_p)}$ with ω given by the onset and the end of the cutoff regions in Fig. 1. To include the influence of the differing effective potentials for the SAE and TAE cases we have inserted for I_p the two corresponding ground-state energies as given in Fig. 2. The fraction of the distribution with the highest momenta is shown to be in between the two arrows in both cases. We find, thus that the differences in the momenta and in the effective ionization potentials at the times of the recollisions of the tunneled jointly explain the difference in the harmonic yield.

We conclude that the total effect of a second active electron oscillating in the vicinity of the ionic core is small if it comes to the high-order regime of harmonic generation via tunneling. Due to the small deviations and uncertainties with respect to the exact position of the cutoff regime, a precise relative analysis of the roles of electron correlation and potential descreening is difficult. However, the main contribution is clearly shown to arise from the dynamical descreening of the significantly moving inner electron as shown earlier in the lower-order regime of harmonic generation.

The authors acknowledge funding from the German Research Foundation (Nachwuchsgruppe within Sonderforschungsbereich 276).

[1] C. J. Joachain *et al.*, Adv. At. Mol. Phys. **42**, 225 (2000); H. Kapteyn and M. Murnane, Phys. World **12**, 31 (1999); T. Brabec and F. Krausz, Rev. Mod. Phys. **72**, 545 (2000); M. Protopapas *et al.*, Rep. Prog. Phys. **60**, 389 (1997).
[2] K. Kulander, Phys. Rev. A **36**, 2726 (1987).
[3] P. B. Corkum, Phys. Rev. Lett. **71**, 1994 (1993).
[4] T. Weber *et al.*, Phys. Rev. Lett. **84**, 443 (2000); R. Moshammer *et al.*, *ibid.* **84**, 447 (2000).
[5] N. Sarukura *et al.*, Phys. Rev. A **43**, 1669 (1991).
[6] J. L. Krause, K. J. Schafer, and K. C. Kulander, Phys. Rev. Lett. **68**, 3535 (1992).
[7] A. Sanpera, P. Jönsson, J. B. Watson, and K. Burnett, Phys. Rev. A **51**, 3148 (1995).
[8] H. Xu, X. Tang, and P. Lambropoulos, Phys. Rev. A **46**, R2225 (1992).
[9] N. Moiseyev and F. Weinhold, Phys. Rev. Lett. **78**, 2100 (1997).
[10] X. M. Tong and S. I. Chu, Phys. Rev. A **57**, 452 (1998).
[11] S. Dionissopoulou, T. Mercouris, and C. A. Nicolaides, Phys. Rev. A **61**, 063402 (2000).
[12] D. G. Lappas, A. Sanpera, J. B. Watson, K. Burnett, P. L. Knight, R. Grobe, and J. H. Eberly, J. Phys. B **29**, L619 (1996).
[13] K. T. Taylor, J. S. Parker, D. Dundas, E. Smyth, and S. Vivirito, in *Multiphoton Processes 1996* (Institute of Physics, Bristol, 1997), p. 56.
[14] S. X. Hu, W. X. Qu, and Z. Z. Xu, Phys. Rev. A **57**, 3770 (1998).
[15] J. Eberly, R. Grobe, C. Law, and Q. Su, in *Atoms in Intense Laser Fields* (Academic Press, New York, 1992), p. 301.
[16] J. Fleck, J. Morris, and M. Feit, Appl. Phys. **10**, 129 (1976).
[17] R. Heather, Comput. Phys. Commun. **63**, 446 (1991).
[18] A. L'Huillier, L. Jönsson, and G. Wendin, Phys. Rev. A **33**, 3938 (1986).
[19] K. C. Kulander, K. J. Schafer, and J. L. Krause, in *Super-Intense Laser-Atom Physics* (Plenum Press, New York, 1993), p. 95.
[20] M. Lewenstein, P. Balcou, M. Ivanov, A. L'Huillier, and P. Corkum, Phys. Rev. A **49**, 2117 (1994).